# Characterization of Ion Dynamics in Structures for Lossless Ion Manipulations

Aleksey V. Tolmachev, Ian K. Webb, Yehia M. Ibrahim, Sandilya V.B. Garimella, Xinyu Zhang, Gordon A. Anderson, and Richard D. Smith*

Biological Sciences Division Pacific Northwest National Laboratory, 3335 Innovation Avenue (K8-98), P.O. Box 999, Richland, Washington 99352, United States

ABSTRACT: Structures for Lossless Ion Manipulation (SLIM) represent a novel class of ion optical devices based upon electrodes patterned on planar surfaces, and relying on a combined action of radiofrequency and DC electric fields and specific buffer gas density conditions. Initial experimental studies have demonstrated the feasibility of the SLIM concept. This report offers an in-depth consideration of key ion dynamics properties in such devices based upon ion optics theory and computational modeling. The SLIM devices investigated are formed by two surfaces, each having an array of radiofrequency (RF) "rung" electrodes, bordered by DC "guard" electrodes. Ion motion is confined by the RF effective potential in the direction orthogonal to the boards and limited or controlled in the transversal direction by the guard DC potentials. Ions can be efficiently trapped and stored in SLIM devices where the confinement of ions can be "soft" in regard to the extent of collisional activation, similarly to RF-only multipole ion guides and traps. The segmentation of the RF rung electrodes and guards along the axis makes it possible to apply static or transient electric field profiles to stimulate ion transfer within a SLIM. In the case of a linear DC gradient applied to RF rungs and guards, a virtually uniform electric field can be created along the axis of the device, enabling high quality ion mobility separations.
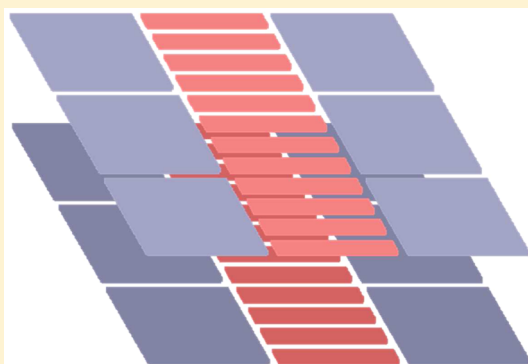
Mass spectrometry (MS) continues its rapid growth as a key technique for analyzing complex chemical and biochemical samples with an increasing array of applications.[1,2] Combining MS with separation techniques, e.g. liquid chromatography or ion mobility spectrometry (IMS), enables analysis of more complex samples. Different combinations can present challenges, due to differences in sample flow rate characteristics, carrier media and/or gas pressure conditions, etc., which often results in throughput and/or sensitivity compromises. We are developing new approaches based upon Structures for Lossless Ion Manipulation (SLIM) that aim at enabling much more complex sequences of ion manipulations in one platform, with potential advantages that include greater speed and reduced sample size requirements. SLIM constitutes a novel class of ion optical devices, relying critically on a combined action of radiofrequency and DC electric fields and specific buffer gas density conditions. The lossless operation, that is, an ability to transmit and store ions with negligible losses, is one of the key attributes of the SLIM concept. The property is inherited, e.g., from the ion funnel and ion funnel trap devices, for which it has been demonstrated both theoretically and in a number of experimental studies.[3-6] Early experimental evidence for the lossless operation included the observation of ion current transmitted though the ion funnel without noticeable losses.[4,5] Such highly efficient transmission is observed over a wide m/z range and can be maintained using a range of RF voltages and frequencies, in line with the theoretically predicted lossless regime characteristics.[3,5] From the ion dynamics perspective, the lossless regime is realized when the potential well exceeds the ion kinetic energy. In the 1 Torr pressure range ions are efficiently thermalized and the potential well sufficient for the lossless operation needs to be significantly higher than the thermal energy, which can be achieved using appropriately chosen electrode configurations.

The SLIM concept introduces the use of DC elements to confine ions, in addition to the assembly of RF electrodes generating the pseudopotential well, as used previously in the ion funnel and related devices, and can greatly increase the versatility of potential devices based upon the approach. In contrast to conventional constant field drift tube[7-9] and traveling wave[10,11] devices, SLIM can potentially be readily assembled into many alternative arrangements. Here, we demonstrate this ability by evaluating a basic building block needed to enable complex manipulations, a linear SLIM component, comprising RF/DC guiding electrodes and DC guard electrodes. Using printed circuit board (PCB) based SLIM allows for a multitude of electrode designs to be rapidly fabricated, tested, and applied at low cost based on the results

of ion trajectory and potential calculations. The SLIM are not fundamentally limited to IMS experiments and can be configured for various pressure environments. We aim to utilize these devices in the future to allow for extended series of ion manipulations of biologically relevant macromolecules and complex mixtures currently unattainable by state-of-the-art instrumentation.

Initial experimental studies have demonstrated the feasibility of the SLIM concept.[12] This report offers an in-depth consideration of the ion dynamics properties of the devices, based on ion optics theory and computer modeling. Ion dynamics theory is applied to analyze the ion motion driven by radiofrequency (RF) and DC electric fields, in a bath gas environment. We begin with analysis of the potential wells generated by SLIM electrodes, considering how various proportions of the device influence the ion focusing properties. Ions transmitted in the SLIM experience combined action of DC electric fields and intense RF fields, which can provide conditions for collisional activation, as we consider next. Further, we explore the ion capacity of a linear section of the SLIM. Finally, we analyze the potential performance of a SLIM configured as an ion mobility spectrometer (IMS).

■ METHODS

The modeling and theoretical approach was originally developed for the simulation driven development and optimization of the ion funnel.[3,5] The SLIM considered in this study is formed by two planar and parallel boards, each having a sequence or RF "rung" electrodes, bordered by DC "guard" electrodes (Figure 1). Ion motion is confined by the RF
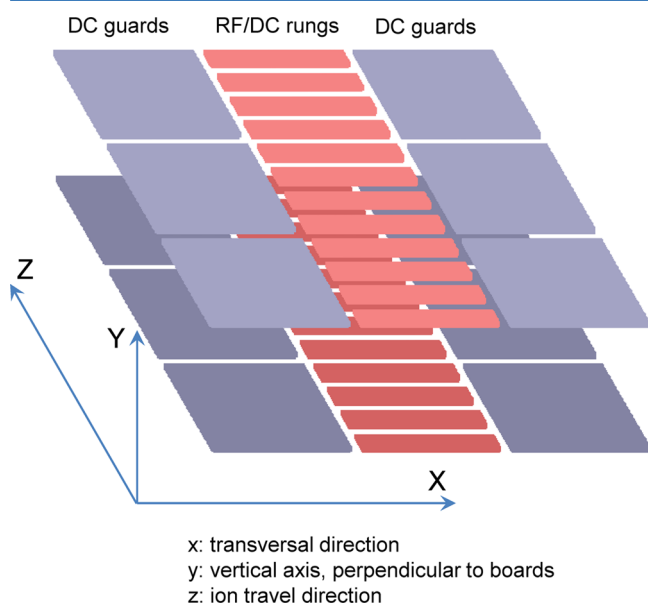

Figure 1. Segment of a Structure for Lossless Ion Manipulation, formed by two planar boards, each having DC guard electrodes and central RF/DC rung electrodes; the coordinate system as used for modeling is shown on the left.

effective potential[13,14] in the direction orthogonal to the boards and is limited by the guard DC potentials in transverse directions. Figure 1 illustrates the coordinate system used in the context of a short SLIM segment. The RF voltages are applied to the rungs with alternating phase on adjacent electrodes. In addition to the RF voltages, the rungs can carry a DC gradient

that can direct ion motion along the Z-axis. Such an arrangement is often implemented in ion funnels and related devices.[3−6] The DC-only guard electrodes limit ion motion in the transversal dimension (i.e., X-axis).

Thus, ion motion in SLIM is driven by a combination of forces produced by the sum of the DC electric field E_{DC} and the effective potential field E_{eff}:

$$F = ze(E_{DC} + E_{eff})$$

Here z is the charge state of the ion, and e is the elementary charge; the total force F, as well as E_{DC} and E_{eff} are 3D vector functions of coordinates X, Y, and Z. The effective potential field E_{eff} is calculated as a gradient of the effective potential V_{eff}, which in turn is a scalar function of coordinates, defined by the local intensity of the RF electric field E_{RF}:[13,14]

$$V_{eff} = \frac{zeE_{RF}^2}{4m\omega^2}$$

The ion mass m is expressed in SI units; the angular frequency ω is related to the RF frequency f (Hz) as $\omega = 2\pi f$. The DC and RF potential distributions can be obtained by solving the Laplace equation, using the DC and RF potentials applied to boundaries shaped as the SLIM electrodes. There is no exact analytical expressions for such geometries; thus, we rely on numerical solutions. The potential calculations reported here are based on a custom developed approach that provides direct potential calculations for complex 3D geometries.[15−17]

■ RESULTS

Effective Potentials in SLIM. The RF field distribution between the two surfaces forming the SLIM is depicted in Figure 2. Equipotential contours in the top portion of Figure 2a show intense electric fields in areas close to rungs; at the plane of symmetry in the center the field intensity is reduced forming a nearly field-free region. The transversal cross section (Figure 2b) shows flat equipotential contours in the center region and negligible field intensity extending beyond the central rungs between guard electrodes. Such a distribution produces steep effective potential wells along RF rung electrodes and a nearly flat potential at midplane. There is no confinement in the X-direction, as opposed to the ion funnel, where circular RF electrodes surround the area of ion drift. In the border between the RF rungs and the guard electrodes, a repulsive force is created which drives ions outward. Opposing this repulsion force is the DC electric field, defined by the DC offset between the guard electrodes and RF rungs. The DC potential can be applied to the guards to constrain ion motion in the X dimension and confine ions in the central region between the arrays of rung electrodes on the opposing surfaces. Two example geometries are considered in Figure 3a, showing the guard DC potential as a function of X. In each case RF/DC rungs are 5.3 mm long and 0.76 mm wide, with separation of 0.76 mm and a DC offset of 10 V applied to the guards. A wider gap between the boards (5.7 mm) leads to an increased penetration of the DC potential to the center, ~2.5 V at the minimum. In the case of a narrow gap (2.7 mm), the central DC potential is reduced to ~0.45 V. The smaller penetration for the narrower gap results in weaker ion focusing in the transversal directions, i.e., a wider area around the center that can be occupied by ions.

Ion density distributions for the SLIM designs considered here will result from the combined action of the DC field from
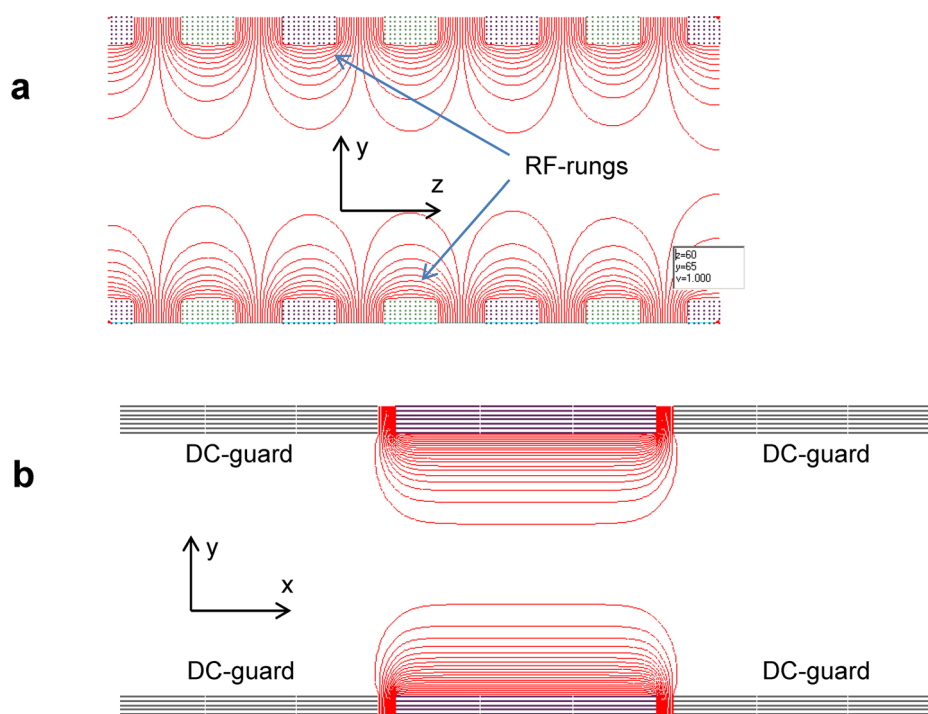
9163

dx.doi.org/10.1021/ac502054p | Anal. Chem. 2014, 86, 9162−9168

Figure 2. Equipotential contours for the RF fields from potentials applied to the central rung electrodes: (a) cross section along the *YZ* plane of symmetry; (b) transversal cross section, *XY* plane.

the guard electrodes and the effective RF focusing generated by the rungs. Figure 3b shows profiles for the combined potential, $V_{eff} + V_{DC}$, as a function of the vertical coordinate (Y). The effective potential V_{eff} was calculated for RF rungs configured as described above, $f = 0.8$ MHz, RF voltage $100V_{p-p}$, m/z 1000. The DC potential at the central plane *YZ* shows a local maximum at the center that is reduced near the surfaces due to increased screening of the external DC field by the rungs. The combined potential can have the local maximum in the center $(Y = 0)$, when the guard DC potential is high enough, so that the local $V_{DC}(Y)$ maximum prevails over the central minimum of the effective potential $V_{eff}(Y)$. A pronounced local maximum is seen in the case of wider gap, 5.7 mm; the "hump" is reduced for 4.2 mm gap and completely removed in the case of narrow gap, 2.7 mm. The configurations in Figure 3b were calculated for rungs 5.3 mm long; when using a wider SLIM configuration having 8.4 mm long rungs, the local maximum was not created for a 4.2 mm gap. However, such a configuration compromises ion focusing in the *X* direction due to a combination of wider rungs and poor penetration of the guard DC field.

A smaller gap, < ~4 mm, has the advantage of a more robust operation with respect to imperfections of the guard potentials, such as created when the guard length covers a number of rungs. Larger gaps, up to 6 mm, require a more precise adjustment of the guard potential, possibly using shorter guards covering fewer rungs, but also have the advantage of better focusing in the direction orthogonal to the ion path. However, the increased penetration of the guard DC field also serves to increase the extent of ion collisional excitation, as discussed next. Based on such considerations, we selected an interboard gap of approximately 5 mm in conjunction with designs having 5.3 × 0.76 mm rungs and 0.76 inter-rung spacing as among those for more detailed theoretical end experimental evaluation.

Collisional Activation of Ions in the SLIM Designs Studied. One initial SLIM implementation has used a spacing

of 4.76 mm between surfaces (to be described in detail elsewhere[12]), which is in line with the optimal gap dimensions for devices with the electrode dimensions discussed above. Ions confined between the surfaces will tend to be localized in two potential wells ~1 mm above and below the midplane (Figure 3b) and separated by a barrier of 0.24 V. While small, the barrier is sufficient in the absence of significant space charge to divide ions into two distinct packets, since the ion density distribution along the vertical (Y) axis is governed by the Boltzmann distribution with the thermal energy (0.025 eV) in the denominator of the exponent.[18,19] This configuration differs from the one encountered in collisional focusing multipoles, with ions occupying an area along the axis of symmetry and where the RF field intensity vanishes.[19] In the current configuration, the DC electric field shifts the ion equilibrium position into a region of nonzero RF field intensity, where some limited collisional activation can occur. The degree of the RF ion heating can be evaluated in terms of the effective temperature:[20]

$$\Delta T_{eff} = \frac{2}{3} \frac{m_g}{m} \frac{zeV_{eff}}{k_B}$$

The ion temperature is increased above the gas temperature by $\Delta T_{eff} = 21$ K, corresponding to only minor collisional activation. The calculation used $m_g = 28$ for the N_2 gas molecular mass, the ion mass and charge $m = 1000$, $z = 1$, and the effective potential at the local minimum $V_{eff} = 0.1$ V. While further optimization of the gap and electrode dimensions can undoubtedly further reduce such effects, we also conclude that the ion confinement by means of the combination of the DC electric field and the RF effective field in the present SLIM configuration provides a viable alternative to RF-only devices, such as RF multipoles.

Ion Charge Capacity for the SLIM Design Studied. The ion charge capacity for SLIM can be estimated based on the
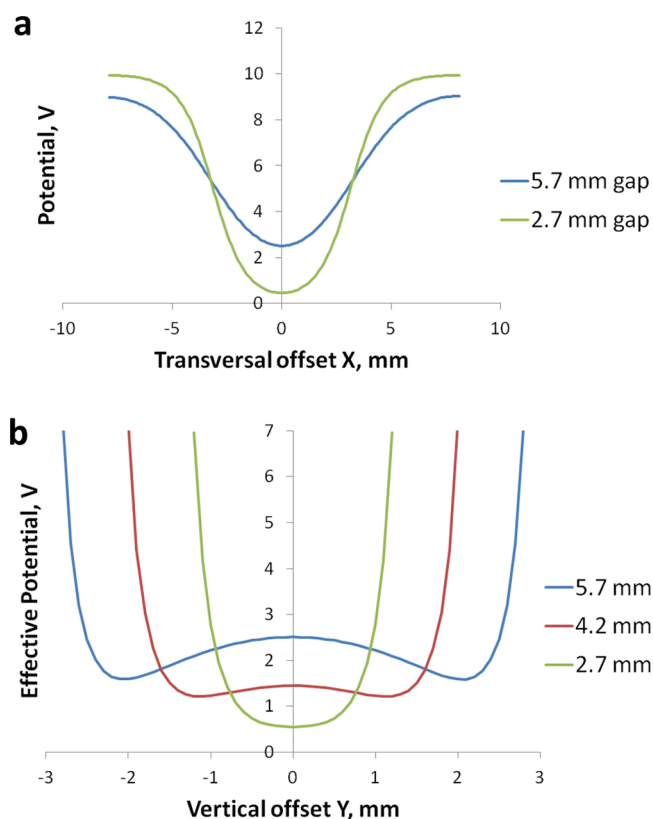
a

b

Figure 3. (a) DC potential profiles for rungs 5.3 mm wide, for either 2.7 mm or 5.7 mm spacing between the SLIM surfaces. The wider gap (5.7 mm) provides tighter focusing in the transverse (X) dimension due to greater penetration of fields from the guard electrodes; (b) SLIM effective potential in the vertical (Y) dimension, at the midplane $X = 0$, for different interboard spacings. A local maximum in the center between boards, $Y = 0$, is increased for wider spacing, 5.7 mm (blue) due to increased field penetration from the DC guards. The local maximum is reduced for 4.2 mm spacing (red) and disappears for the smaller 2.7 mm spacing (green).

opposing forces of Coulombic repulsion and that due to the DC electric field and effective RF field generated from the potential applied to the SLIM electrodes. Figure 4 shows electric fields balancing the Coulomb repulsion of the stored ion charge. The electric field produced by the stored ions is balanced by the DC electric field from guard electrodes, E_{DC}, plus the field E_{eff} due to the effective potential generated by RF electrodes, with the ion population split into two strips, aligned
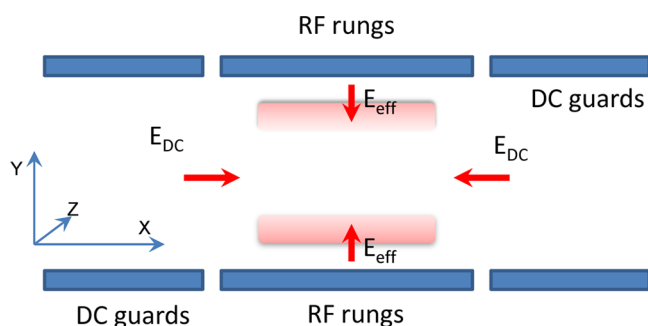

Figure 4. Storage of ions in the SLIM. The Coulomb repulsion forces are balanced by the DC electric field produced by guard electrodes and the RF effective focusing field from RF rung electrodes.

as noted above. The effective field orthogonal to the electrodes confines Coulombic driven expansion in the Y-direction. The field produced by DC guards contributes to the vertical (Y) component with the opposite sign, slightly reducing the RF effective focusing. Figure 5a shows transversal (X) profiles of the vertical (Y) components of the DC electric field and the RF effective field, calculated based on 3D potential modeling, using parameters of the trapping experiment:[21] RF frequency 2.4 MHz, RF voltage 165 Vpp, ions m/z 466.3, singly charged, and the DC guard offset 6.6 V. The total confining field (solid curve, Figure 5a) reaches 18.7 V/cm in the center ($X = 0$), and decreases to 12.5 V/cm approaching the sides of the RF rungs at $X = \pm 2$ mm. The E_y profiles in Figure 5a were calculated for a vertical position $Y = 1.8$ mm from the midplane, corresponding to efficient confinement from the sides. Figure 5b shows vertical (Y) profiles of the horizontal fields E_x, confining the stored ion charge from the sides, plotted for the vertical XZ plane at $X = 2$ mm, bordering the range of Y-confinement in Figure 5a. The total of two x-fields (solid curve in Figure 5b) reaches a maximum of 11.8 V/cm at $y = \pm 1.5$ mm and declines steeply for vertical offsets above 2 mm. The decline of X-confinement at high vertical positions is due to two factors: the DC field screened by the rungs and the RF effective field acting to eject ions from the area of high effective potential close to RF rungs. As a result, the vertical expansion of the ion cloud is effectively limited at $Y < \approx 2$ mm; further expansion leads to leakage of ions through the reduced x-barriers at the sides. Accordingly, the total stored ion charge Q can be estimated based on the confining field intensity, using Gauss's relationship:

$$F_E = Q/\varepsilon_0$$

Here ε_0 is the electric constant; the electric field flux F_E is defined as an integral of the field produced by the stored charge over a closed surrounding surface.[22] Considering the two-dimensional approximation, the electric field flux is estimated as

$$F_E = 2\Delta x \Delta z E_y$$

where Δx and Δz are the x and z dimensions of a rectangular area of the stored charge; the Coulomb field E_y is counter-balanced by the total field in Figure 5a. The total number of elementary charges stored in the SLIM segment would be

$$N_e = Q/e = 2\varepsilon_0 \Delta x \Delta z E_y/e \approx 1 \times 10^8$$

The X-range used for the estimation is $\Delta x = 4$ mm; the length of the trapped charge region is equal to the length of the trapping SLIM segment, $\Delta z = 15.24$ cm; electric field $E_y = 15$ V/cm corresponds to experimental conditions, as evaluated above (Figure 5a).

The estimated charge capacity agrees with that observed in initial experiments using a linear SLIM segment to trap ions,[21] and is among the highest stored charge amounts reported. The ion funnel trap used with IMS is capable of storing up to 10^7 elementary charges.[23] In terms of the linear charge density, the value obtained, $Q_z \sim 10^{-10}$ C/m, compares favorably with the charge capacity of RF multipoles.[24] The ability of the device to create the DC field gradient to stimulate a ion transport along the axis can be used to achieve significant ion currents; e.g., for the field $E_z \sim 40$ V/cm, the ion velocity $v_z \sim 100$ m/s, and the ion current is $i = Q_z v_z \sim 10$ nA, corresponding to the high end of use in MS with, e.g., ESI or MALDI sources.
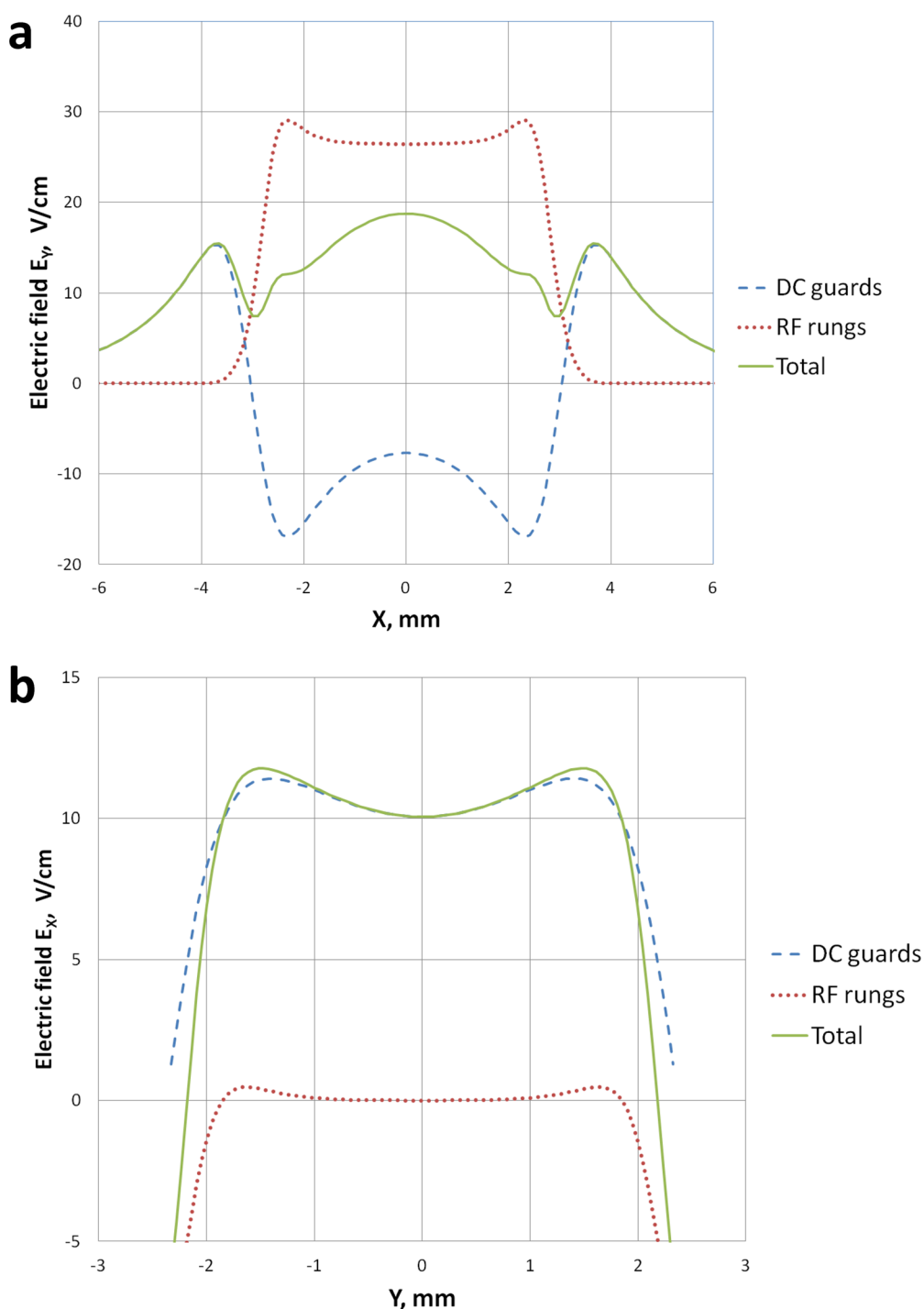
Figure 5. Electric field confining stored ion charge (a) in the vertical dimension, Y-components, and (b) in the horizontal dimension, X-components. The DC electric field produced by the guard electrodes (dashed), effective potential field from RF rung electrodes (dotted), and a sum of the two fields (solid).

Potential for Ion Mobility Separations in SLIM. As discussed above, ions can be efficiently trapped and stored in SLIM devices; the confinement of ions can be "soft" with respect to collisional activation, similar to RF-only multipole ion guides and traps. An additional functionality of SLIM is provided by the segmentation of the RF rung electrodes and guards along the Z axis resulting in electric field profiles that will stimulate ion motion. We consider a basic case of a DC linear gradient applied to RF rungs and guards, such that a virtually uniform electric field E_z is created along the axis of the

device. Considering the elevated pressure, > ~1 Torr nitrogen bath gas, the ion motion stimulated by the electric field represents a drift with a constant velocity, defined by the ion mobility K:[25]

$$v_{drift} = KE_z$$

The pressure conditions are similar to IMS-TOF MS platforms incorporating electrodynamic ion funnels[23,26,27] with an ion drift region, in the form of a drift tube, where a constant and uniform electric field and a bath gas having
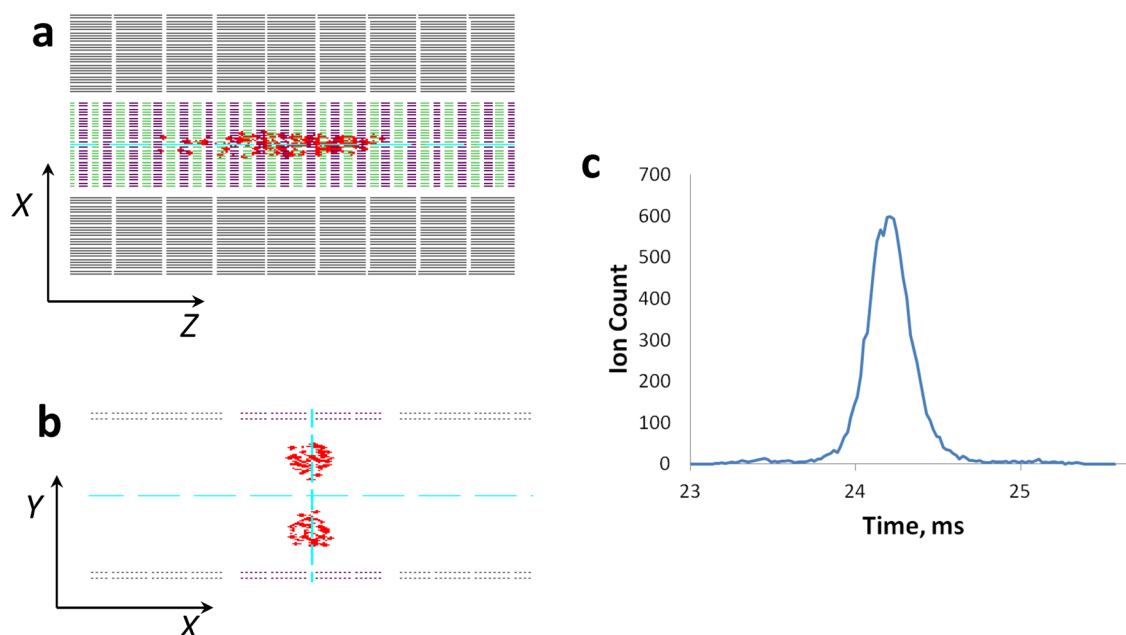

Figure 6. Modeling the ion mobility separation in a linear SLIM segment. Ion density distribution for a pulse of ions in a horizontal *XZ* projection (a), vertical *XY* planar projection (b), and calculated ion arrival time distribution (c).

negligible flow velocity provide conditions for the ion drift according to the above equation.[7−9] In the case of a linear SLIM segment having a constant axial field, the ion cloud is shaped by confining fields, the effective RF focusing in the vertical dimension, and DC electric fields generated by the guard electrodes.

A computer model of the ion motion has been implemented to analyze details of the ion motion in such a configuration (Figure 6). Ions form into two elongated packets, each occupying a local *Y*-potential well (Figure 3b). The ion density distribution along the *Z*-axis takes the form of a Gaussian having the exponential width defined by diffusion. The vertical split is orthogonal to the ion drift and does not affect the Gaussian arrival time distribution (Figure 6c).

The ion drift time and IMS resolving power have been modeled for conditions of an initial experimental study[12] for ions of *m/z* 922. The ion cross section was measured independently using the IMS TOF instrument[27] and used to calculate the ion mobility for 4.1 Torr nitrogen, at 298 K, the conditions employed in our experimental study.[12] The ion drift time vs electric field intensity shows a close agreement between the model and experiment.[12,28] The IMS resolving power in Figure 7 has been modeled for the guard DC offset of 5 V, the same as experiment, and for an increased offset of 40 V. For the lower offset, 5 V, modeling results approach the theoretical IMS resolving power for low electric fields and trend lower for higher fields. Modeling results for the increased guard offset of 40 V show a resolving power profile noticeably lower than the theoretical one across the range of electric fields. This can be explained considering the axial variations of the effective potential, which contribute to the temporal dispersion of ions, when the increased DC field drives ions closer to RF electrodes. We conclude that the RF field and irregularities of the DC gradient do not degrade the quality of IMS measurements in SLIM when reasonably optimal conditions are chosen. This is supported by the initial experimental study showing SLIM IMS resolving power closely matching theoretical calculations.[12,28]
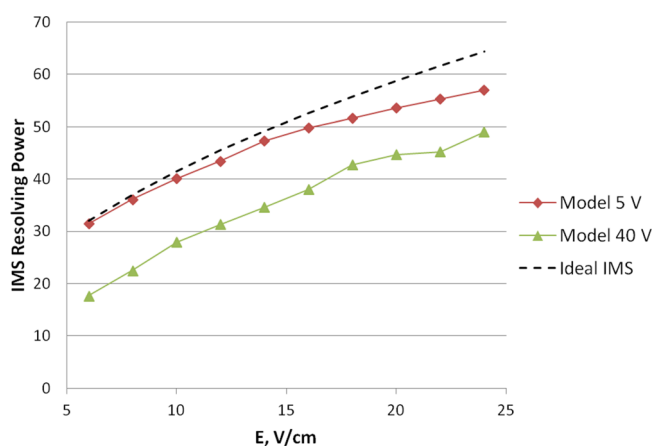

Figure 7. Ion mobility resolving power as a function of electric field intensity. Modeling results for the guard offset 5 V (diamonds), offset 40 V (triangles), and calculated assuming the ideal IMS drift tube (dashed).

We also note that mobility separations using transient DC fields (e.g., traveling waves) are similarly feasible.

■ CONCLUSIONS

The ion confinement in SLIM is accomplished by a combination of the effective potential generated by the RF rung electrodes, and DC potential offset from the guard electrodes. The relative sizes of the electrodes, applied voltages, and surface spacing have been initially optimized for ion confinement conditions. Potential calculations have been applied to analyze the RF and DC potential profiles for various SLIM geometries. Configurations having rung electrode lengths significantly shorter than the separation between boards display a significant penetration of the guard DC potential into the central volume. This creates conditions for ion packets such that they can be split into two volumes. Alternatively,

geometries with smaller interboard gaps produce a single, nonsplit ion packet extended in the transversal direction.

Ions confined in SLIM experience combined effects of the DC electric and RF fields, which create conditions for potentially sustained collisional activation. For the optimal geometry and moderate guard potentials, however, only very minor collisional ion activation is produced, with the effective ion temperature increased above the bath gas temperature by ~10 K. In this respect, SLIM provide a viable alternative to the RF-only multipole ion guides and traps, with negligible collisional activation of ions.

The ion capacity of a linear section of the present SLIM design is estimated to be ~10^8 elementary charges for a section 10 cm long, an ion population among the highest achievable in ion traps.

Computer modeling of ion motion supports the lossless ion transmission for the SLIM configurations studied. A precise modeling of the ion diffusion inside a linear drift region supports the capability for high quality ion mobility measurements using SLIM, a finding that we experimentally confirm elsewhere.[12,28] Overall, the SLIM ion dynamics modeling study is consistent with initial experimental observations, as well as the observation of efficient ion transmission in IMS experiments, and with the lossless ion trapping and storage extending to high ion populations, up to 10^8 ions, and for significantly extended times, ≫1 s.[21]

■ AUTHOR INFORMATION

Corresponding Author
*E-mail: rds@pnnl.gov.

Notes
The authors declare no competing financial interest.

■ ACKNOWLEDGMENTS

■ REFERENCES

(1) Chait, B. T. *Annu. Rev. Biochem.* **2011**, *80*, 239−246.
(2) Angel, T. E.; Aryal, U. K.; Hengel, S. M.; Baker, E. S.; Kelly, R. T.; Robinson, E. W.; Smith, R. D. *Chem. Soc. Rev.* **2012**, *41*, 3912−3928.
(3) Tolmachev, A. V.; Kim, T.; Udseth, H. R.; Smith, R. D.; Bailey, T. H.; Futrell, J. H. *Int. J. Mass Spectrom.* **2000**, *203*, 31−47.
(4) Kim, T.; Tolmachev, A. V.; Harkewicz, R.; Prior, D. C.; Anderson, G. A.; Udseth, H. R.; Smith, R. D.; Bailey, T. H.; Rakov, S.; Futrell, J. H. *Anal. Chem.* **2000**, *72*, 2247−2255.
(5) Page, J. S.; Tolmachev, A. V.; Tang, K.; Smith, R. D. *J. Am. Soc. Mass Spectrom.* **2006**, *17*, 586−592.
(6) Kelly, R. T.; Tolmachev, A. V.; Page, J. S.; Tang, K.; Smith, R. D. *Mass Spectrom. Rev.* **2009**, 1−19.
(7) Bowers, M. T.; Kemper, P. R.; von Helden, G.; van Koppen, P. A. M. *Science* **1993**, *260*, 1446−1451.
(8) Clemmer, D. E.; Jarrold, M. F. *J. Mass Spectrom.* **1997**, *32*, 577−592.
(9) Eiceman, G. A.; Karpas, Z. *Ion Mobility Spectrometry*, 2nd ed.; CRC Press: Boca Raton, FL, 2005.
(10) Giles, K.; Pringle, S. D.; Worthington, K. R.; Little, D.; Wildgoose, J. L.; Bateman, R. H. *Rapid Commun. Mass Spectrom.* **2004**, *18*, 2401.
(11) Giles, K.; Williams, J. P.; Campuzano, I. *Rapid Commun. Mass Spectrom.* **2011**, *25*, 1559.
(12) Webb, I. K.; Garimella, S.; Tolmachev, A. V.; Zhang, X.; Chen, T.; Norheim, R. V.; Anderson, G. A.; Ibrahim, Y. M.; Smith, R. D. *Anal. Chem.* **2014**, DOI: 10.1021/ac502055e.
(13) Dehmelt, H. G. *Adv. Atom Mol. Phys.* **1967**, *3*, 53−290.
(14) Gerlich, D. In *State Selected and State-to-State Ion−Molecule Reaction Dynamics. Part 1. Experiment*; Ng, C. Y., Baer, M, Eds.; Wiley: New York, 1992; Vol. *LXXXII*; pp 1−176.
(15) Tolmachev, A. V.; Robinson, E. W.; Wu, S.; Smith, R. D.; Paša-Tolić, L. *J. Am. Soc. Mass Spectrom.* **2011**, *22*, 1334−1342.
(16) Tolmachev, A. V.; Robinson, E. W.; Wu, S.; Smith, R. D.; Futrell, J. H.; Paša-Tolić, L. *J. Am. Soc. Mass Spectrom.* **2012**, *23*, 1169−1172.
(17) Tolmachev, A. V.; Robinson, E. W.; Wu, S.; Smith, R. D.; Leach, F. E.; Futrell, J. H.; Paša-Tolić, L. *Int. J. Mass Spectrom.* **2012**, *325*, 45−50.
(18) Tolmachev, A. V.; Chernushevich, I. V.; Dodonov, A. F.; Standing, K. G. *Nucl. Instrum. Methods B* **1997**, *124* (1), 112−119.
(19) Tolmachev, A. V.; Udseth, H. R.; Smith, R. D. *Int. J. Mass Spec.* **2003**, *222*, 155−174.
(20) Tolmachev, A. V.; Vilkov, A. N.; Bogdanov, B.; Paša-Tolić, L.; Masselon, C. D.; Smith, R. D. *J. Am. Soc. Mass Spectrom.* **2004**, *15*, 1616−1628.
(21) Zhang, X.; Garimella, S.; Prost, S. A.; Webb, I. K.; Chen, T.; Tang, K.; Tolmachev, A. V.; Norheim, R. V.; LaMarche, B. L.; Danielson, W. F., 3rd; Baker, E. S.; Anderson, G. A.; Ibrahim, Y. M.; Smith, R. D. An Initial Evaluation of Ion Traps in Structures for Lossless Ion Manipulation (SLIM) at a High Pressure: Ion Storage, Ion Accumulation and Ion Ejection. *Anal. Chem.* (in preparation).
(22) Grant, I. S.; Phillips, W. R. In *Electromagnetism*, 2nd ed.; Manchester Physics Series; John Wiley & Sons: 2008; ISBN 978-0-471-92712-9.
(23) Tolmachev, A. V.; Clowers, B. H.; Belov, M. E.; Smith, R. D. *Anal. Chem.* **2009**, *81*, 4778−4787.
(24) Tolmachev, A. V.; Udseth, H. R.; Smith, R. D. *Anal. Chem.* **2000**, *72*, 970−978.
(25) Mason, E. A.; McDaniel, E. W. *Transport Properties of Ions in Gases*; Wiley: New York, 1988.
(26) Tang, K.; Shvartsburg, A. A.; Lee, H. N.; Prior, D. C.; Buschbach, M. A.; Li, F.; Tolmachev, A. V.; Anderson, G. A.; Smith, R. D. *Anal. Chem.* **2005**, *77*, 3330−3339.
(27) Baker, E. S.; Clowers, B. H.; Li, F.; Tang, K.; Tolmachev, A. V.; Prior, D. C.; Belov, M. E.; Smith, R. D. *J. Am. Soc. Mass Spectrom.* **2007**, *18*, 1176−1187.
(28) Sandilya, V. B.Garimella, S. V. B.; Ibrahim, Y. M.; Webb, I. K.; Tolmachev, A. V.; Zhang, X.; Anderson, G. A.; Smith, R. D.; . Simulation of Electric Potentials and Ion Motion in Planar Electrode Structures for Lossless Ion Manipulations (SLIM). *J. Am. Soc. Mass Spectrom.*, accepted for publication.